Ternary fission fragment yields analysis in $^{124}Sn+^{112,124}Sn$ at 26*A* MeV reaction

J. Gauthier, M. Barbui, X.G. Cao, K. Hagel, J.B. Natowitz, R. Wada, and S. Wuenschel

An analysis of the data set coming from 26*A* MeV ^{124}Sn on ^{112}Sn and ^{124}Sn targets acquired by the NIMROD heavy ion detector [1] is underway and almost ready for publication. These data are being used to perform studies of the emission sources [2] with emphasis on emission of fragments in ternary fission processes [3] at high temperature and excitation energy. A better understanding of this phenomenon should help to improve the characterization of the reaction dynamics [4], especially in the low density mid-rapidity region.

The data set is composed of 33 runs combining 26 000 000 events. Charge identification is achieved up to Z=42 and isotopic identification is achieved up to Z=14 with very low statistics of mass identified fragments for charges above Z=9. The energy calibration of the Si-CsI(Tl) is now done. We used the SRIM calculation [5] and a Si-Si punch-through-energy based calibration to fit the energy distributions in all detectors. The energies resulting from the calibration are in very good agreement with those predicted by the HIPSE event generator [6] which gives us additional confidence in the calibration technique. Unfortunately, the absence of light particle calibration points prevents us from calibrating the light particles (Z=1,2) in the CsI(Tl).

The starting point of this analysis is based on the work done in reference [3]. About 0.3% of heavy nucleus spontaneous fissions produce a third fragment coming from the low density neck region [7]. Most of those fragments are α particles. A high yield of tritons relative to protons is observed as shown in reference [8] and the yield of heavier fragments decreases with Z. To reproduce the yields, we have previously used a nucleation model together with the nuclear statistical equilibrium (NSE) code LIBNUCEQ [9]. The NSE model is based on the assumption that the chemical potential μ(Z,A) is governed by equation (1). The yields are then extracted by the use of equation (2) which takes into account the temperature, the density and the proton fraction number

$$\mu(Z,A) = Z\mu_p + (A-Z)\mu_n, \qquad (1)$$

$$\mu(Z,A) = m(Z,A)c^2 + kT\ln\left\{\frac{\rho N_A Y(Z,A)}{G(Z,A)}\left[\frac{h^2}{2\pi m(Z,A)kT}\right]^{3/2}\right\}. \quad (2)$$

This approach is in good agreement with experimental yields of light ternary fragments from spontaneous fission of ^{241}Pu but overestimates the yields of heavier isotopes as we can see in reference [3]. The inclusion of the nucleation process [10] allows us to modulate the approach to equilibrium. The nucleation uses surface tension constraints and the chemical potential to grow or diminish cluster size by accepting or emitting a single nucleon as time evolves. The nucleon absorption/emission process is driven by the critical cluster size A_c that is viewed as the mass threshold at which the clusters grow or break down. The inclusion of this process, which takes into account the reaction time and is described by equations 3, 4 and 5, greatly improves the agreement with the experimental data as it is shown in reference [3].

$$Y(A,\tau) = \frac{1}{2}\rho \exp\left[-\frac{G(A)}{T}\right] \times \operatorname{erfc}\left\{B(T,\sigma)\frac{[(A/A_c)^{1/3} - 1] + \left(1 - A_c^{-1/3}\right)\exp(-\tau)}{\sqrt{1-\exp(-2\tau)}}\right\} \quad (3)$$

$$B(T,\sigma) = 2R_0\left(\frac{\pi\sigma}{T}\right)^{1/2} A_c^{1/3} \quad (4)$$

$$\tau = \frac{3.967c\rho}{A_c^{2/3}\sqrt{T}}t \quad (5)$$

In order to pursue such studies at higher temperature we turned to symmetric nuclear reactions. The mid-rapidity emission in the 26*A* MeV ^{124}Sn + $^{112,\,124}$Sn system collisions allows us to prepare heavy systems similar to those which undergo spontaneous fission, thus to probe the neck emission process at higher temperature. In this analysis, the ternary-like-fragments are selected using the relative angle between the fragment of interest and the Z_{max} in the center of mass reference frame (see drawing in Fig. 2). To select mid-peripheral and peripheral collision, we apply a cut on $Z_{max} > 20$ as shown in Fig. 1.

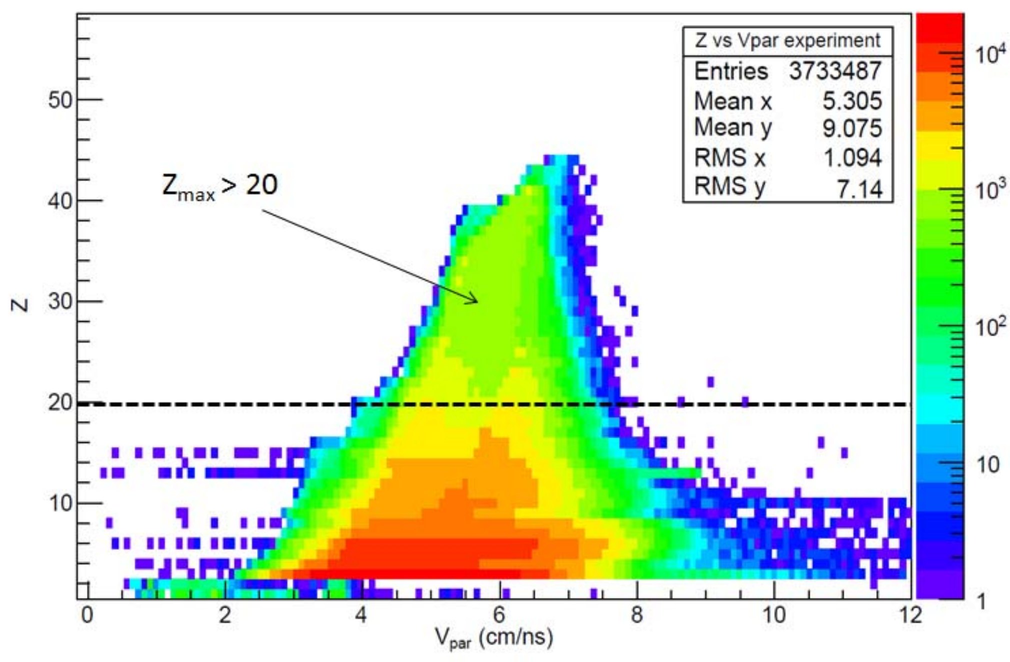

FIG. 1. Z_{max} selection as a function of the parallel velocity.

The ternary-like-fragment relative angle has to be as close as possible to 90° in the center of mass frame but since the statistics are limited, we need to do a compromise between the relative angle selection and the number of events within this selection. To do so, we select the relative angle interval for which the average energy of the particles in the center of mass stops decreasing. This should exclude projectile-like emission sources. Fig. 2 shows these distributions for Z=3, 4 and 5. The compromise relative angle selection chosen corresponds to 50-130°.

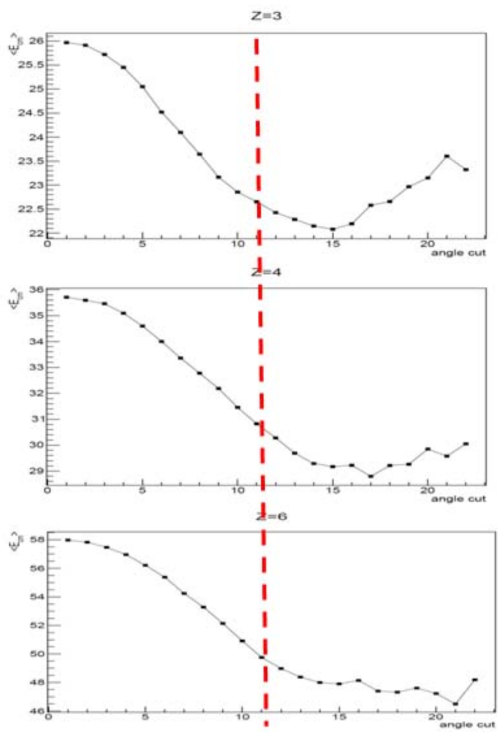

Cut #	rel. angle min	rel. angel max
1	0	180
2	5	175
3	10	170
4	15	165
5	20	160
6	25	155
7	30	150
8	35	145
9	40	140
10	45	135
11	50	130
12	55	125
13	60	120
14	65	115
15	70	110
16	75	105
17	80	100
18	82	98
19	84	96
20	86	94
21	88	92
22	89	91

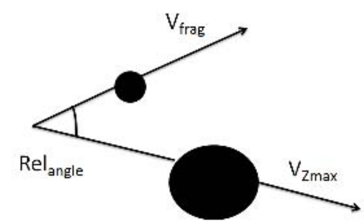

FIG. 2. (left) Average energy in the center of mass for several relative angle selections. The selection (cut) numbers are described in the table (middle). The best compromise is the 50-130° range. (right) Graphical representation of our relative angle definition.

After normalization, we can compare the results of the NSE+nucleation calculation with the experimental data by using the fit metric described in equation (6), which is an average of the discrepancy between the experimental and theoretical *P(Z, A)* points and tells us how well the model reproduces the experimental values.

$$\text{Fit Metric} = \quad M^2 = \sum_j \{\ln[P_{\mathrm{TF}}^{\exp}(Z_j, A_j)] - \ln[P_{TF}(Z_j, A_j)]\}^2 / n \qquad (6)$$

In reference [3], The Fit Metric for spontaneous fission with NSE only (without nucleation) is 4.28 and the one with nucleation included is 1.18. With the NIMROD data presented in Fig. 3, we achieved a M^2 equal to 0.92 for the ^{124} Sn and 0.94 for the ^{112}Sn target. However, these NIMROD fit metric numbers don't take into account the charges above 9 since the number of particles coming from

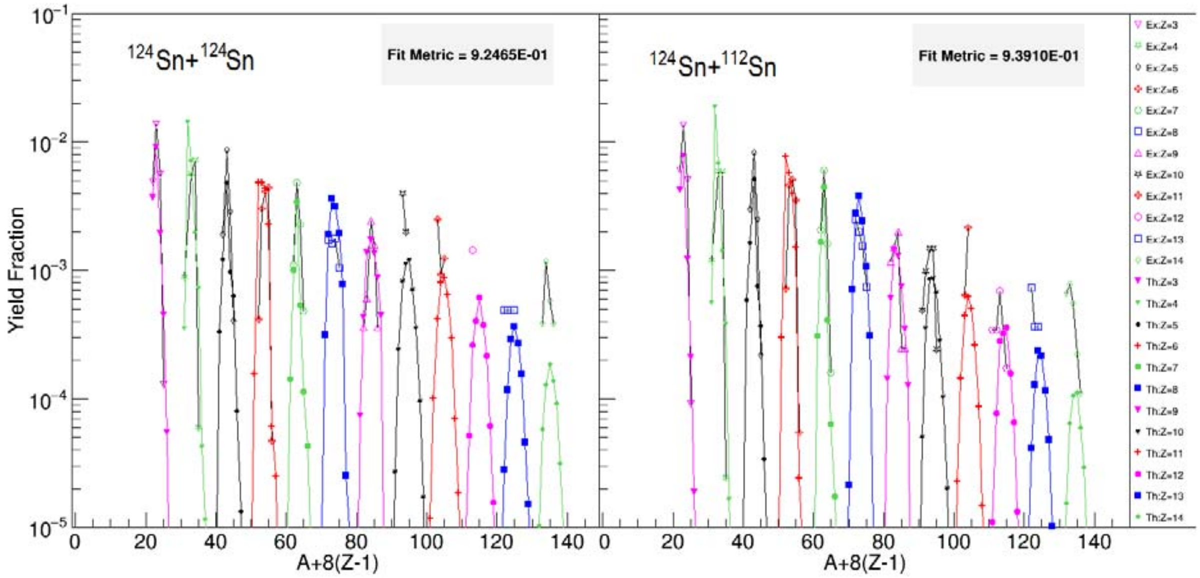

FIG. 3. Fitting results with NIMROD data for both systems with isotopic identification.

the mass identified set is too low for those elements and are then statistically irrelevant. If we don't take into account the isotopic information, meaning that we assign an average mass to each fragment not isotopically identified, the statistics gets much higher and we can reach an even better fit metric value(including all elements) as shown in Fig. 3. In Table I, we present a summary of the fit parameters used to achieve the optimized metric. The temperatures and densities are, as expected, higher than those in reference [3]. In order to achieve the best fit, we have to greatly increase the critical cluster size. The large discrepancies for the heavier isotopes is due to the very low statistics in the mass identified fragments for Z > 9. The discrepancies and values in table 1 still need to be interpreted.

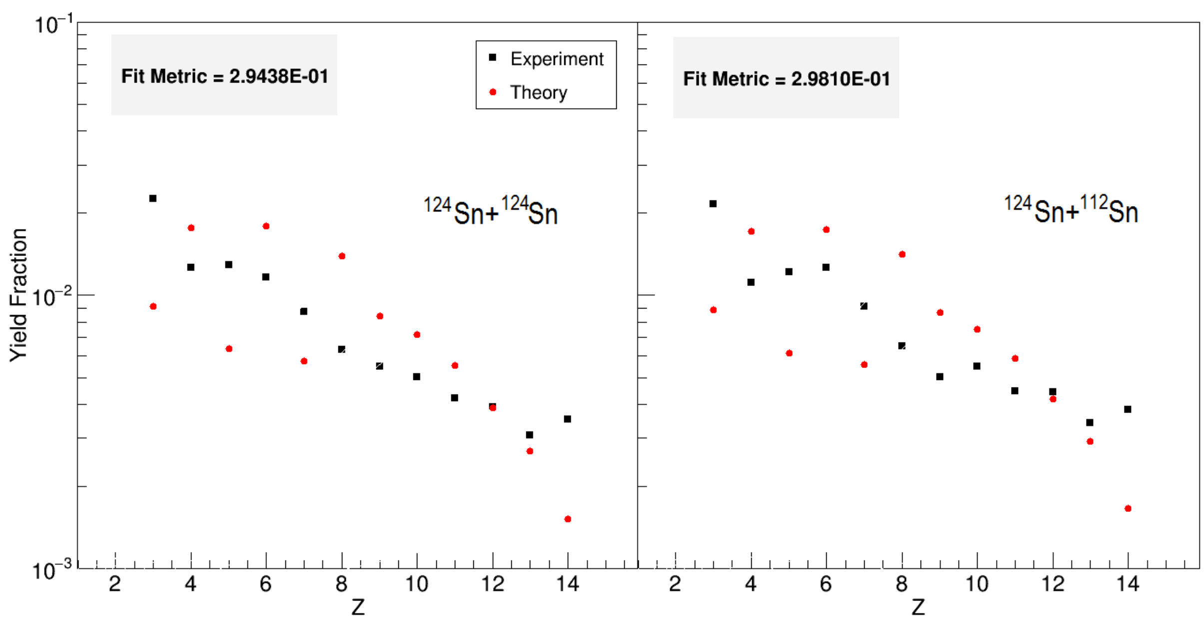

FIG. 4. Fitting results with NIMROD data for both systems with charge identification only.

Table I. Fit parameters for both studied systems including isotopic and Z only selections. The spontaneous fission of ^{241}Pu parameters from reference [3] are also added for comparison. For clarification, the last column, labeled *A*, is a fit performed with the mass only without taking Z into account (still from reference [3]).

System	^{124}Sn+^{124}Sn		^{124}Sn+^{112}Sn		^{241}Pu	
selection	Isotopic	Z	Isotopic	Z	Isotopic	A
temperature (MeV)	2.49	2.30	2.45	2.30	1.4	1.4
density (10^{-4} fm^{-3})	13.0	13.4	12.6	13.7	4	4
time (fm/c)	9200	9300	8400	9400	6400	6400
A_c	16.0	16.0	15.8	16.0	5.4	5.4
proton ratio	0.41	0.41	0.44	0.41	0.34	0.34
fit metric	**0.925**	**0.294**	**0.939**	**0.298**	**1.18**	**0.561**

We would like to thank A.B. McIntosh and S.J. Yennello for the helpful discussions and comments about this work.

[1] S. Wuenschel *et al.*, Nucl. Instrum Methods Phys. Res. **A604**, 578 (2009).
[2] D.V. Shetty *et al*., Phys. Rev. C **68**, 054605 (2003).
[3] S. Wuenschel *et al.*, Phys. Rev. C **90**, 011601, (2014).
[4] M.A. Famiano *et al.*, Phys. Rev. Lett. **97**, 052701 (2006).
[5] J.F. Ziegler *et al.*, Nucl. Instrum. Methods Phys. Res. **B268**, 11 (2010).
[6] D. Lacroix et *al.*, Phys. Rev. C **69**, 054604, (2004).
[7] C. Wagemans, *The Nuclear Fission Process* (CRC Press, Boca Raton, 1991).
[8] A. Schubert *et al.*, Z. Phys. A **341**, 481 (1992).
[9] http://sourceforge.net/p/libnuceq
[10] P. Demo and Z. Kozisek, J. Phys. G **23**, 971 (1997).